Integrated optical interferometers for quantum information applications

Andrea Crespi
Dipartimento di Fisica – Politecnico di Milano
Istituto di Fotonica e Nanotecnologie – Consiglio Nazionale delle Ricerche (IFN-CNR)

CNR IFN Istituto di Fotonica e Nanotecnologie

POLITECNICO MILANO 1863

(multi)-purpose of this talk

Lay the basis of qubit encoding on single photons.

Introduce the fundamentals of single photon manipulation with linear optics…

…in particular adopting an integrated approach based on optical waveguides.

CNR IFN

POLITECNICO MILANO 1863

Bring a few examples, based on the research work conducted here in Milano at IFN-CNR and Politecnico.

Outline

1. Photons and qubits
2. Integrated quantum photonics
3. Computing with linear optics
4. Boson sampling: a route to show quantum advantage

Quantization of the electromagnetic field and encoding of qubits on photons

The very beginning

Planck's black-body theory (1900)

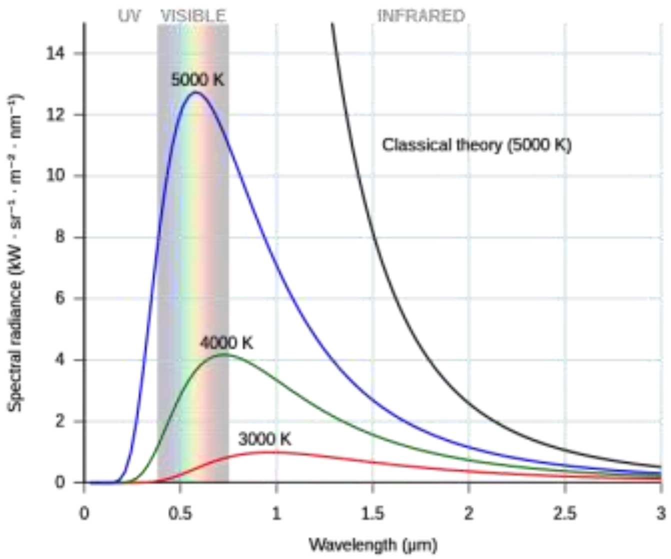

Einstein's theory of photo-electric effect (1905)

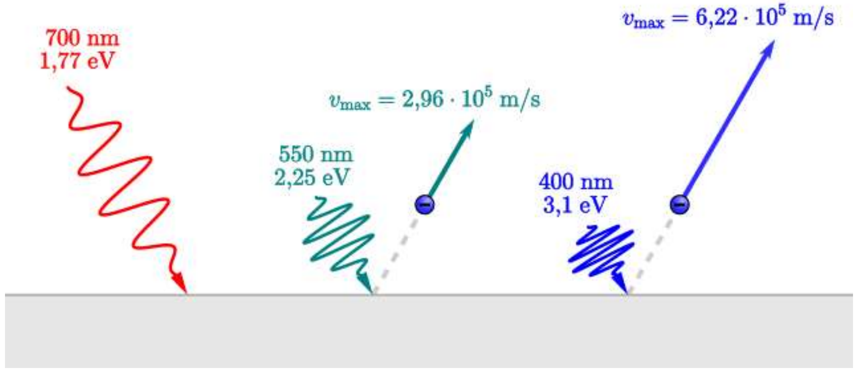

Compton scattering (1923)

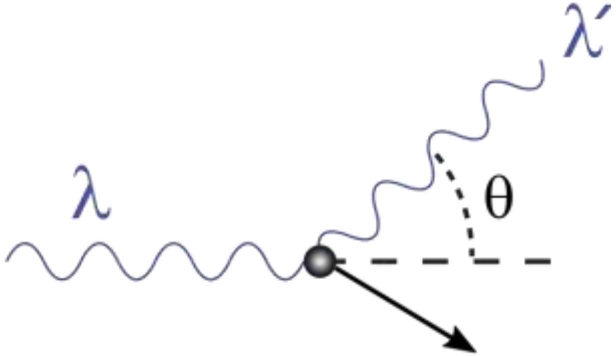

PHOTON

$$E = \hbar\omega \qquad \vec{p} = \hbar\vec{k}$$

theoretical developments followed by Dirac, Glauber and so on....

Harmonic oscillators

CLASSICAL HARMONIC OSCILLATOR

energy $E = \frac{1}{2m} p^2 + \frac{1}{2} m\,\omega^2 x^2 = \frac{1}{2m} |\alpha|^2 = \frac{\alpha\,\alpha^* + \alpha^* \alpha}{4m}$

position $x(t) = \mathrm{A}\ \cos\omega t = \frac{1}{m\,\omega} \frac{\alpha+\alpha^*}{2}$

momentum $p(t) = m\frac{dx}{dt} = -m\omega A\ \sin\omega t = \frac{\alpha-\alpha^*}{2j}$

normal variable $\alpha(t) = m\omega x(t) + jp(t)$

$$\alpha(t) = m\omega A\, e^{-j\omega t} = \alpha(0) e^{-j\omega t}$$

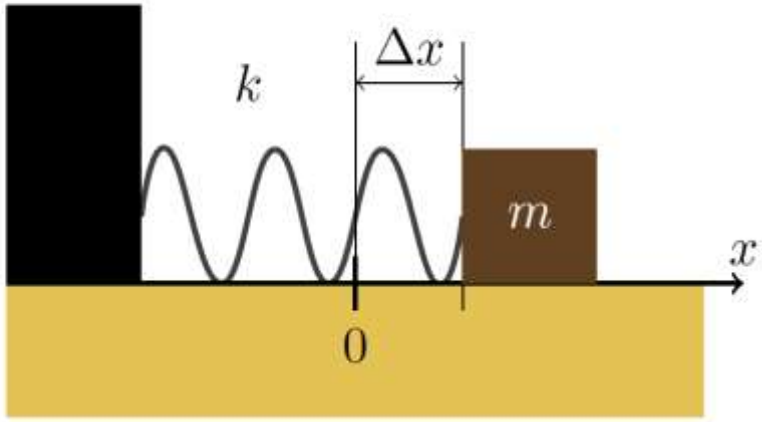

complex oscillation in time!

QUANTUM HARMONIC OSCILLATOR

Hamiltonian $\hat{H} = \frac{\hbar\omega}{2}\left(\hat{a}^\dagger \hat{a} + \hat{a}\hat{a}^\dagger\right)$

position $\hat{x} = \sqrt{\frac{2\hbar}{m\,\omega}}\left(\frac{\hat{a} + \hat{a}^\dagger}{2}\right)$

momentum $\hat{p} = \sqrt{2m\hbar\omega}\left(\frac{\hat{a} - \hat{a}^\dagger}{2j}\right)$

$$\left[\hat{a}, \hat{a}^\dagger\right] = 1$$

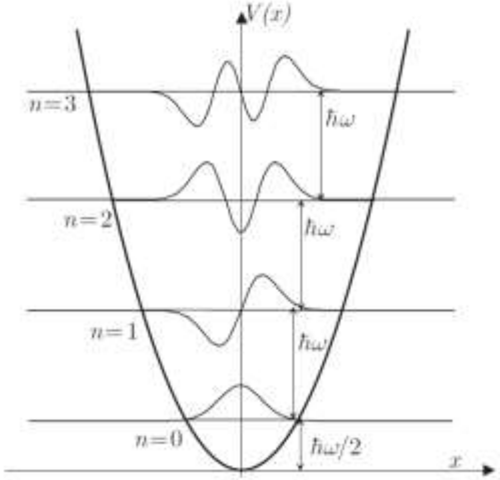

It works by replacing
$\alpha \leftrightarrow \hat{a} \quad \alpha^* \leftrightarrow \hat{a}^\dagger$
apart from a normalization constant.

Electromagnetic modes

In the free space without currents or charges, by employing the vector potential $\vec{A}$, we write:

$$\vec{E} = -\frac{\partial \vec{A}}{\partial t} \quad \vec{B} = \vec{\nabla} \times \vec{A} \qquad\qquad \nabla^2 \vec{A} + \mu_0 \varepsilon_0 \frac{\partial^2 \vec{A}}{\partial t^2} = 0$$

We look for a solution by the separation of variables, namely we look for solutions as:

polarization vector

$$\vec{A} = \mathcal{A}_0 \cdot f(\vec{r}) \cdot \alpha(t) \cdot \vec{\epsilon}$$

normalization constant carrying the measurement units

adimensional function of spatial coordinates (normalized)

adimensional function of time, carrying the field amplitude

We may then combine pairs of solutions (complex conjugated) to make them real:

$$\vec{A} = \mathcal{A}_0 \, \vec{\epsilon} \, [f(\vec{r}) \cdot \alpha(t) + f^*(\vec{r}) \cdot \alpha^*(t)]$$

The time-dependent part shows complex oscillations as an harmonic oscillator:

$$\frac{\partial^2}{\partial t^2} \alpha(t) + \omega^2 \alpha(t) = 0$$

$$\boxed{\alpha(t) = \alpha(0) e^{-j\omega t}}$$

The spatial part is a solution of the Helmholtz equation:

$$\nabla^2 f(\vec{r}) + \mu_0 \varepsilon_0 \omega^2 f(\vec{r}) = 0$$

In the free space and a cubic normalization volume, they can be plane waves.

$$f(\vec{r}) = e^{j \vec{k} \cdot \vec{r}}$$

Applying the oscillator formalism

All relevant fields are written as linear combinations of $\alpha(t)$ and $\alpha^*(t)$

$$\vec{A} = \frac{\mathcal{E}_0}{\omega}\,\vec{\epsilon}\,[f(\vec{r})\cdot\alpha(t) + f^*(\vec{r})\cdot\alpha^*(t)]$$

$$\vec{E} = \frac{\partial\vec{A}}{\partial t} = j\mathcal{E}_0\vec{\epsilon}\,[f(\vec{r})\cdot\alpha(t) - f^*(\vec{r})\cdot\alpha^*(t)]$$

$$\vec{B} = \vec{\nabla}\times\vec{A} = \cdots$$

$$\boxed{\alpha(t) = \alpha(0)e^{-j\omega t}}$$

It is further possible to show that:

$$U = \iiint \left[\tfrac{1}{2}\varepsilon_0|\vec{E}|^2 + \tfrac{1}{2\mu_0}|\vec{B}|^2\right]dV \propto |\alpha|^2$$

And that different modes α_ω give independent energy contributions:

$$\boxed{U = \sum U_l = \sum c_l|\alpha_l|^2}$$

$$\hat{\vec{A}} = \frac{\mathcal{E}_0}{\omega}\,\vec{\epsilon}\left[f(\vec{r})\hat{a} + f^*(\vec{r})\,\hat{a}^\dagger\right]$$

$$\hat{\vec{E}} = j\mathcal{E}_0\vec{\epsilon}\left[f(\vec{r})\hat{a} - f^*(\vec{r})\,\hat{a}^\dagger\right]$$

$$\hat{H} = \hbar\omega\left(\hat{a}^\dagger\hat{a} + \tfrac{1}{2}\right)$$

$$\hat{H}_{tot} = \sum\hbar\omega_l\left(\hat{a}_l{}^\dagger\hat{a}_l + \tfrac{1}{2}\right)$$

Formal similarity with an ensemble of independent classical harmonic oscillators. We associate a quantum harmonic oscillator to each mode, by replacing:

$$\boxed{\alpha \leftrightarrow \hat{a} \quad \alpha^* \leftrightarrow \hat{a}^\dagger}$$

The Fock states

A **photon** is a **quantum of excitation** of a given electromagnetic mode.

"number" operator

$$\hat{H} = \hbar\omega\left(\hat{a}^\dagger\hat{a} + \tfrac{1}{2}\right) = \hbar\omega\left(\hat{n} + \tfrac{1}{2}\right)$$

$$\hat{H}|n\rangle = \hbar\omega\left(n + \tfrac{1}{2}\right)|n\rangle$$

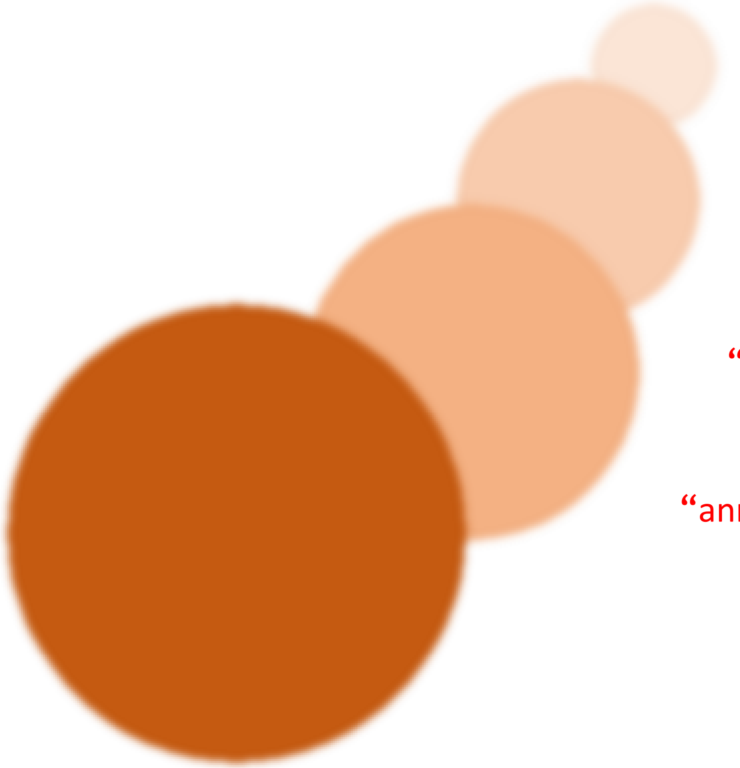

The eigenstates of the single-mode field Hamiltonian are the Fock states $\{|n\rangle\}$, i.e. states with a fixed number of excitations.

$$\langle n|m\rangle = \delta_{nm}$$

They are orthonormal

"creation" operator

"annihilation" operator

$$\begin{cases} \hat{a}^\dagger|n\rangle = \sqrt{n+1}|n+1\rangle \\ \hat{a}|n\rangle = \sqrt{n}|n-1\rangle \\ \hat{a}|\emptyset\rangle = 0 \end{cases}$$

$$|n\rangle = \frac{\left(\hat{a}^\dagger\right)^n}{\sqrt{n!}}|\emptyset\rangle$$

They can be constructed from the vacuum applying repeatedly the $\hat{a}^\dagger$ operator.

Photonic qubits (1)

The generic state of a qubit is a superposition of the 0 and 1 states.

$$|\psi\rangle = c_0|\mathbf{0}\rangle + c_1|\mathbf{1}\rangle \qquad |c_0|^2 + |c_1|^2 = 1$$

In photonic implementations, the two states are **two different modes** of the electromagnetic field.

One photonic qubit is encoded as a **single-photon** state where the single photon is in a superposition of the two modes.

$$|\psi\rangle = \left(c_0\,\hat{a}_{\mathbf{0}}{}^{\dagger} + c_1\,\hat{a}_{\mathbf{1}}{}^{\dagger}\right)|\emptyset\rangle$$

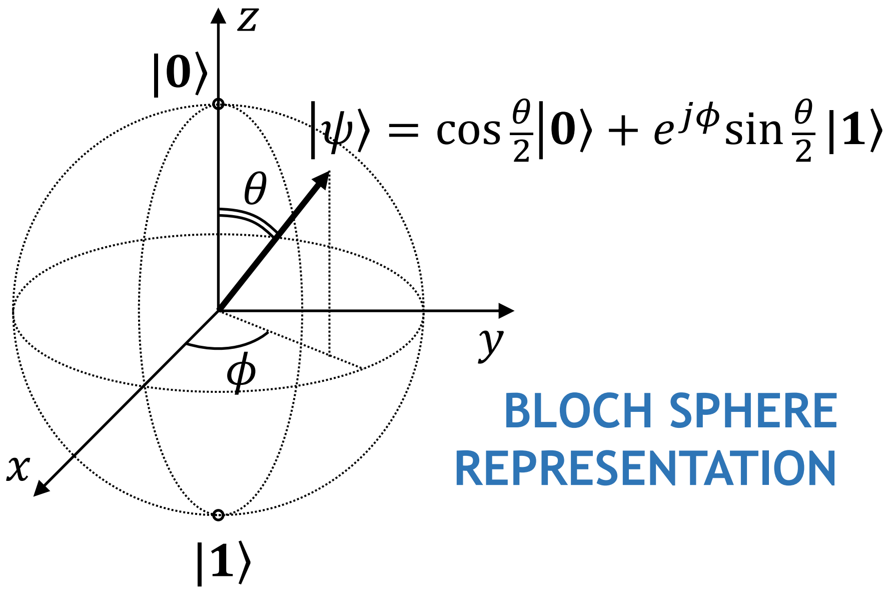

BLOCH SPHERE REPRESENTATION

PATH ENCODING

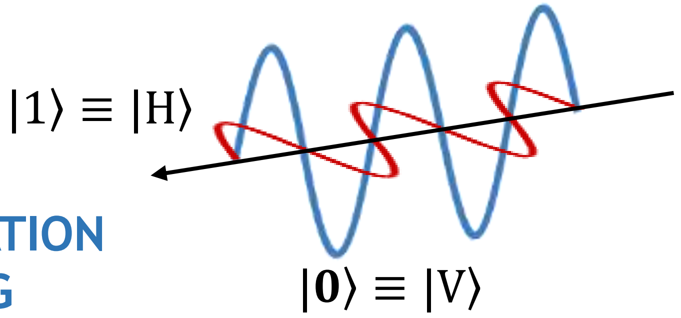

POLARIZATION ENCODING

Photonic qubits (2)

NOTES ON POLARIZATION QUBIT ENCODING

Two orthogonal polarization states (e.g. horizontal and vertical) may be used as computational basis.

$$|\psi\rangle = c_{\mathrm{H}}\underbrace{|\mathbf{H}\rangle}_{|\mathbf{0}\rangle} + c_{\mathrm{V}}\underbrace{|\mathbf{V}\rangle}_{|\mathbf{1}\rangle}$$

The qubit state is described as a 2D complex vector: it is analogous to the **Jones vector** of the polarization state.

$$|\psi\rangle \equiv \begin{bmatrix} c_{\mathrm{H}} \\ c_{\mathrm{V}} \end{bmatrix}$$

Polarization rotations are single-qubit transformations… **single qubit gates**!

A measurement of $\hat{\sigma}_z$ is performed with a polarization beam splitter (PBS) and two single-photon detectors.

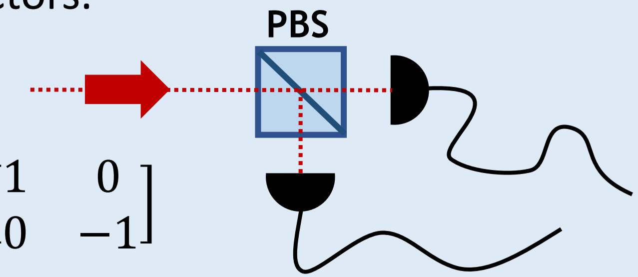

$$\hat{\sigma}_z = \begin{bmatrix} 1 & 0 \\ 0 & -1 \end{bmatrix}$$

A measurement of a generic $\hat{\sigma}_{\vec{u}}$ needs birefringent elements (half- and quarter-waveplates) before the PBS

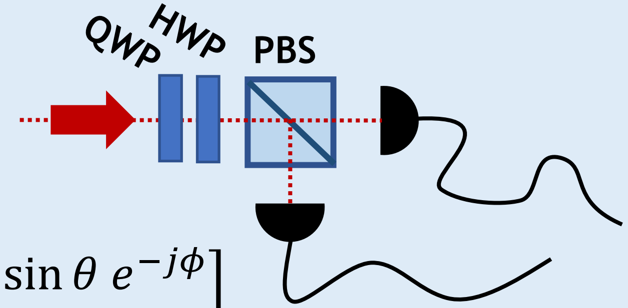

$$\hat{\sigma}_{\vec{u}} = \begin{bmatrix} \cos\theta & \sin\theta\, e^{-j\phi} \\ \sin\theta\, e^{j\phi} & -\cos\theta \end{bmatrix}$$

Outline

1. Photons and qubits
2. Integrated quantum photonics
3. Computing with linear optics
4. Boson sampling: a route to show quantum advantage

Why integrated optics; and what we do in Milano.

Optical waveguides

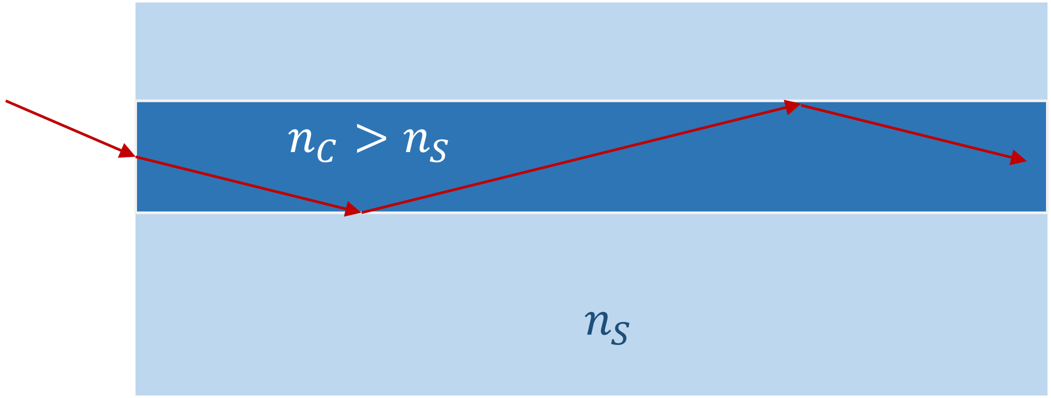

- Dielectric waveguides are transparent structures with a refractive index higher than the surrounding substrate. **Light is confined by total internal reflection.**

- Structures with suitable (small) size may support a **single spatial mode** (two polarizations) of the light at a given wavelength.

Example of silica-on-silicon chip structure for single-mode waveguides @804 nm

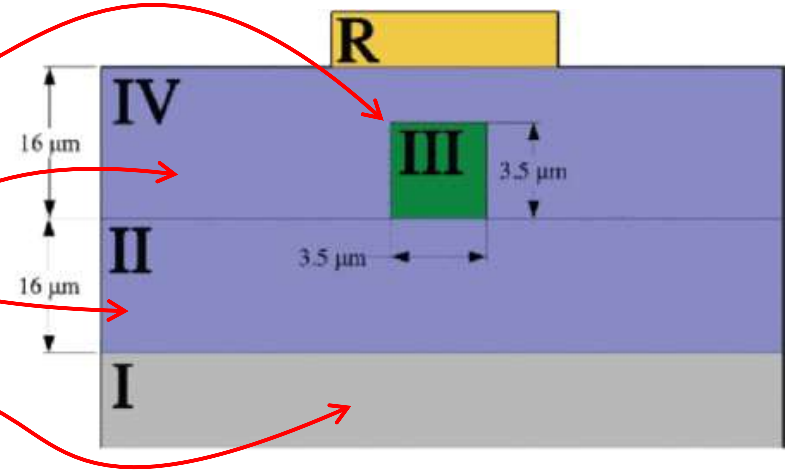

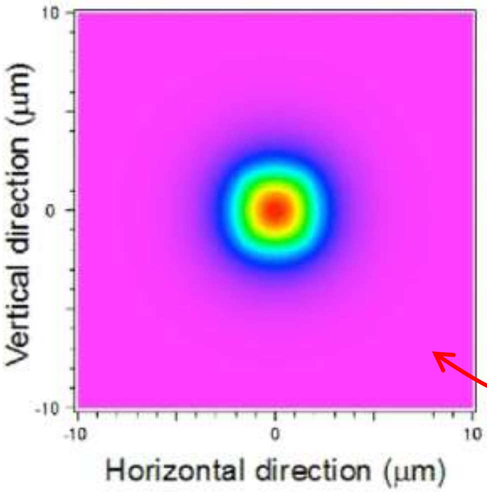

A. Politi *et al.* "Integrated Quantum Photonics" IEEE J. Sel. Top. Quantum Electron. 15, 1673 - 1684 (2009).

A quantum photonic platform

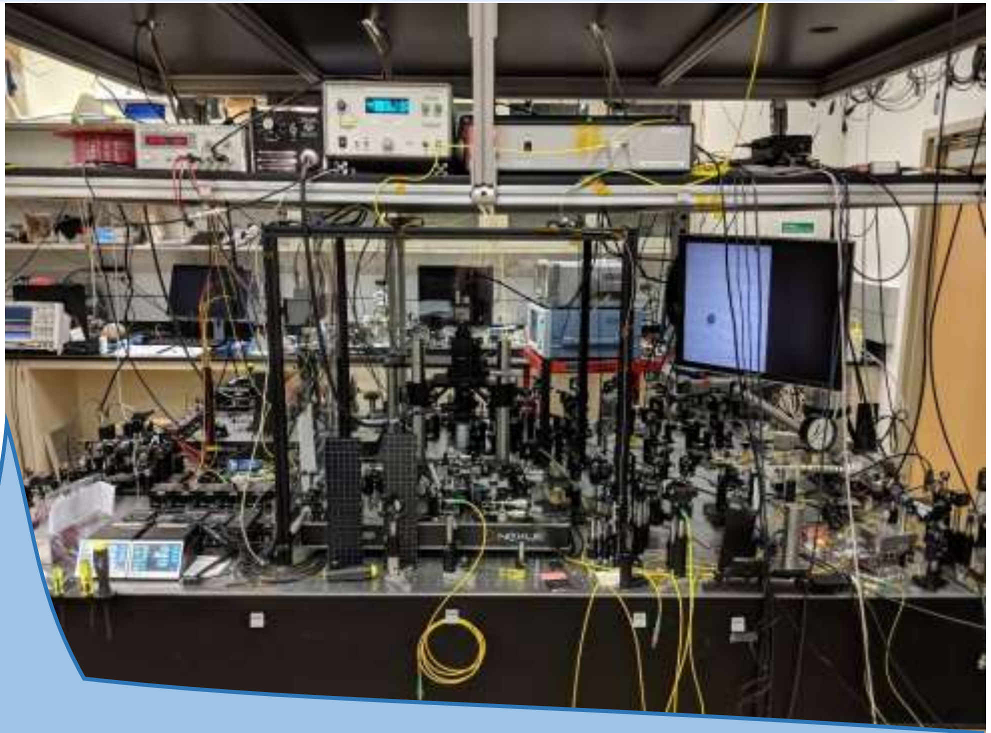

- **Waveguide circuits** allow to control the spatial propagation of **optical modes**, and perform **controlled interactions** between them.
- **Single photon manipulation is possible.** A pair of $\hat{a}$ and $\hat{a}^\dagger$ operators are associated to each mode.
- Complex optical operations can be achieved in a very **compact footprint**: the rise of integrated quantum photonics.

A. Politi *et al*. "Silica-on-silicon waveguide quantum circuits" *Science* 320, 646-649 (2008).

J. Carolan *et al*. "Universal linear optics." *Science* 349, 711-716 (2015).

E. Pelucchi *et al*. "The potential and global outlook of integrated photonics for quantum technologies" *Nat. Rev. Phys.* 4, 194–208 (2022).

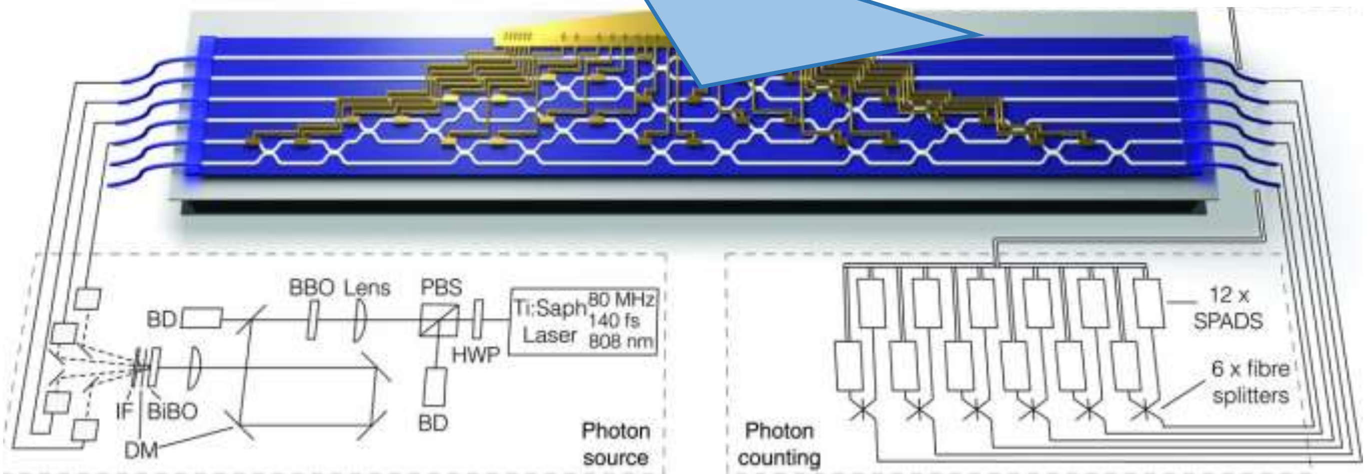

fs laser waveguide writing (1)

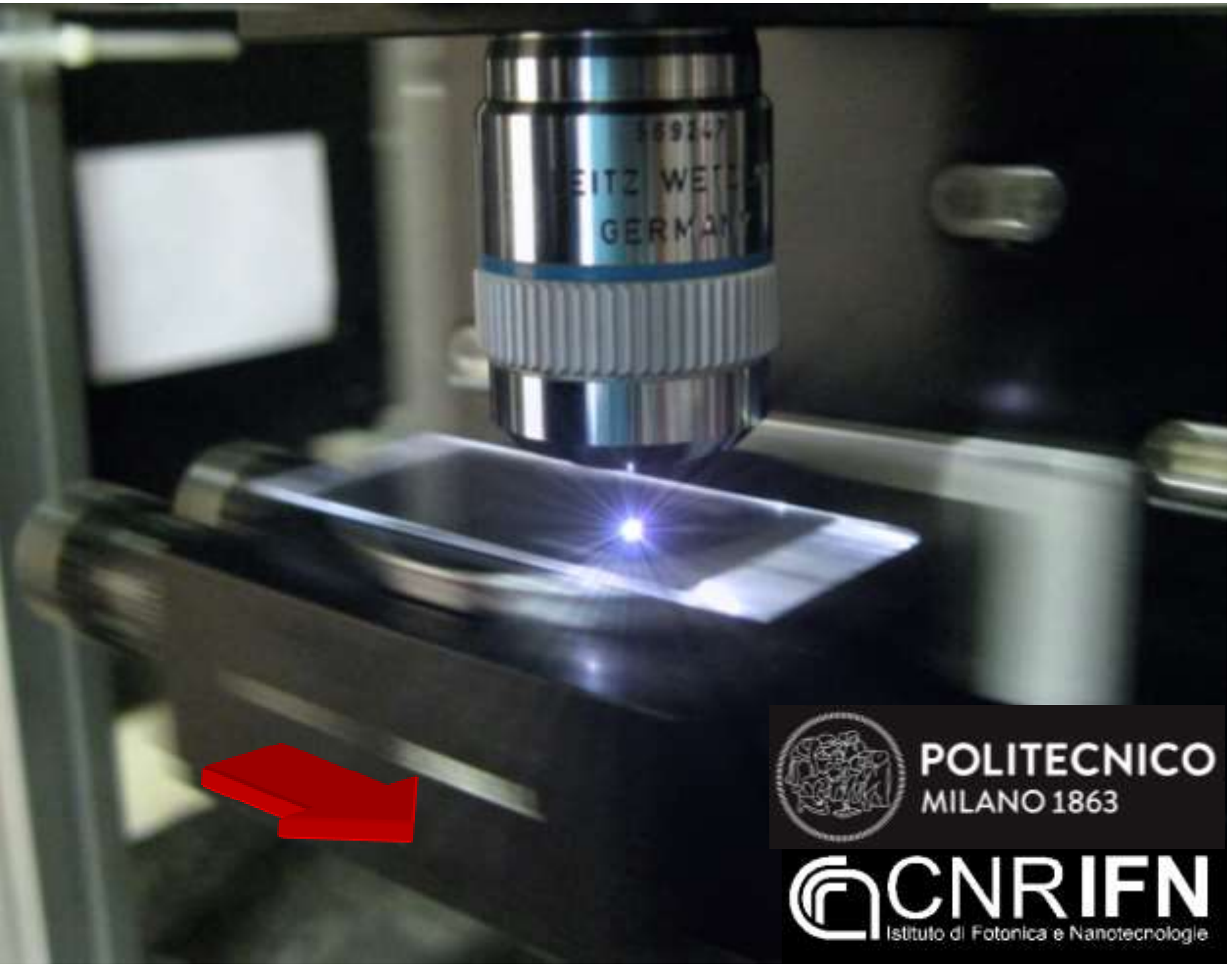

Femtosecond laser pulses are focused in the bulk of a transparent, dielectric material.

- Nonlinear absorption generates a seed of free electrons, multiplied by avalanche.
- Energy transfer to the lattice causes a permanent and localized refractive index modification.
- Thermal accumulation effects can occur at high repetition rates.

Buried optical waveguides are directly fabricated by translation of the sample along the desired path.

G. Corrielli, A. Crespi & R. Osellame. "Femtosecond laser micromachining for integrated quantum photonics." *Nanophotonics* 10, 3789-3812 (2021).

fs laser waveguide writing (2)

Unique capability to fabricate waveguide circuits and arrays in three-dimensions.

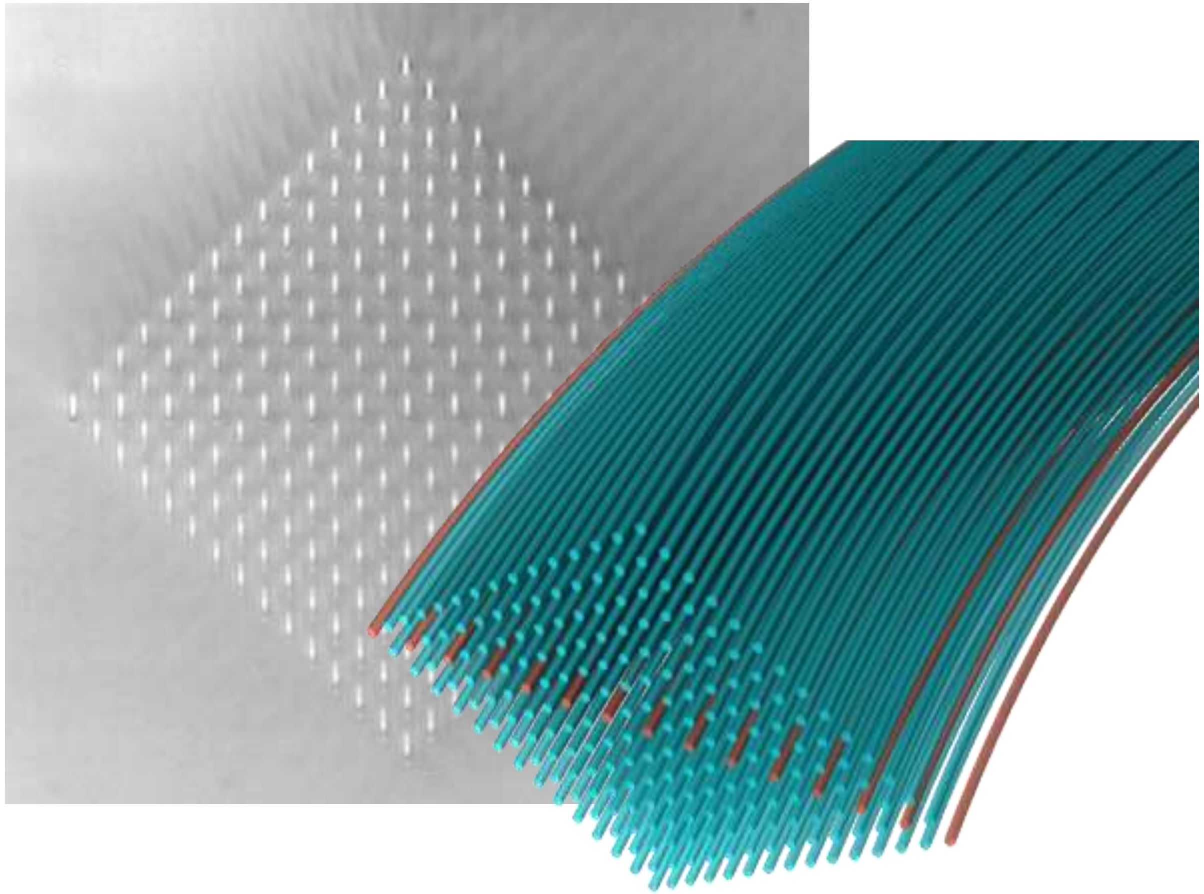

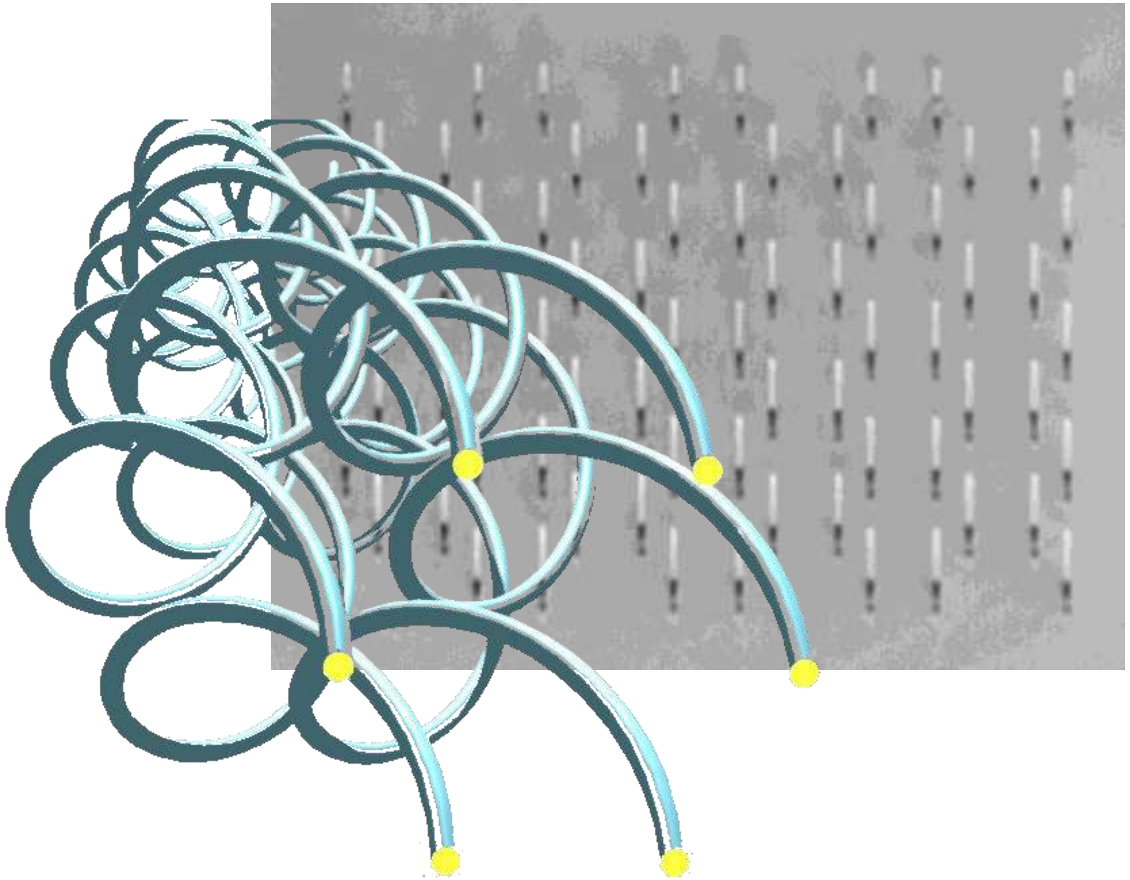

Crespi et al. New J. Phys. 15, 013012 (2013).
Corrielli et al. Nat. Commun. 4, 1555 (2013).

Example: integrated waveplates (1)

A MICROFABRICATION TECHNIQUE WITH UNIQUE CAPABILITIES…

FOCUSING GEOMETRY

MODIFICATION IN THE MATERIAL (WAVEGUIDE)

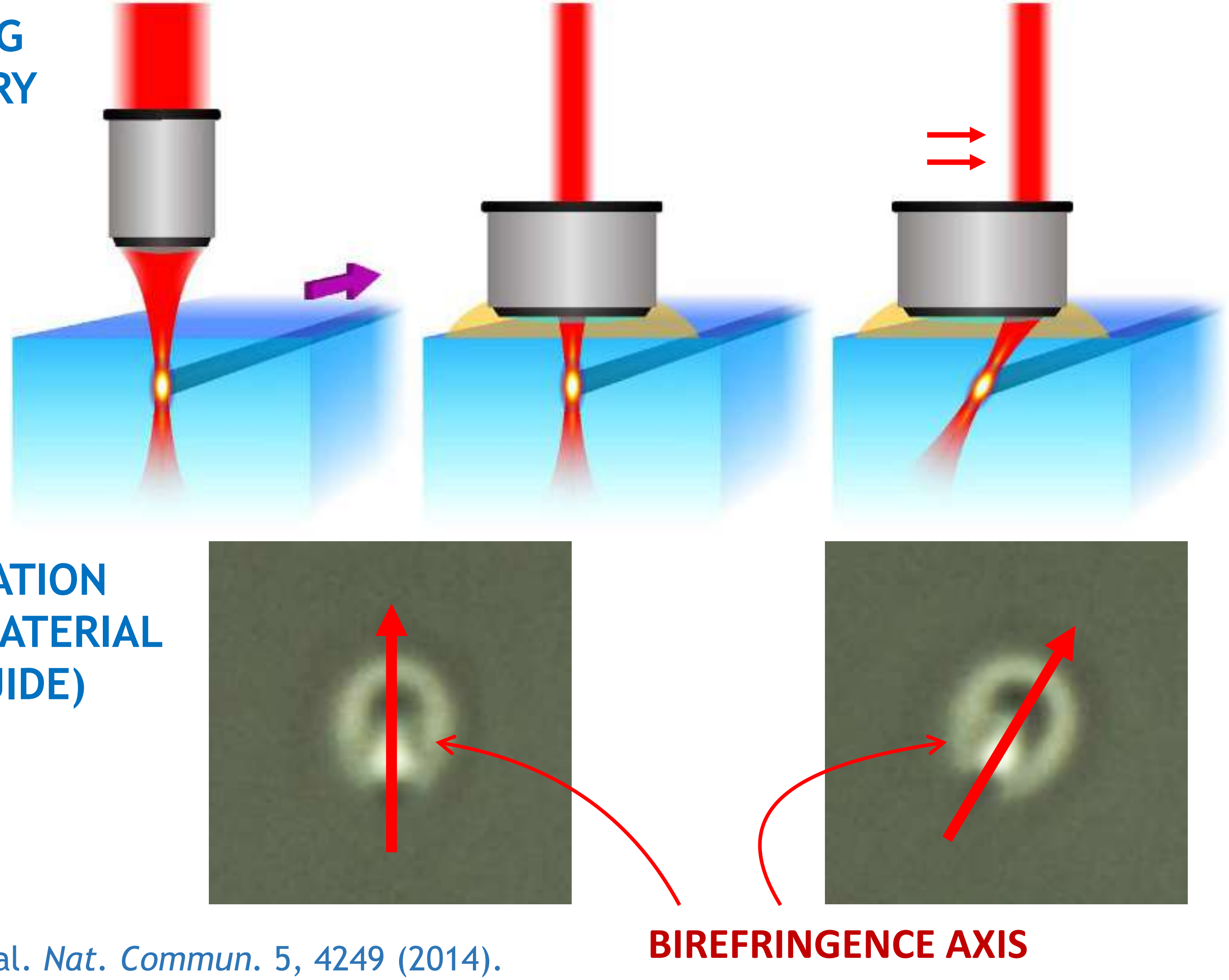

- Femtosecond laser written waveguides have a **natural birefringence** due to anisotropy of the irradiation process.
- A proper focusing apparatus can inscribe waveguide with a tilted symmetry axis.

Namely, a tilted birefringence axis.

G. Corrielli, et al. *Nat. Commun.* 5, 4249 (2014).

Example: integrated waveplates (2)

JOINING TWO WAVEGUIDE SEGMENTS

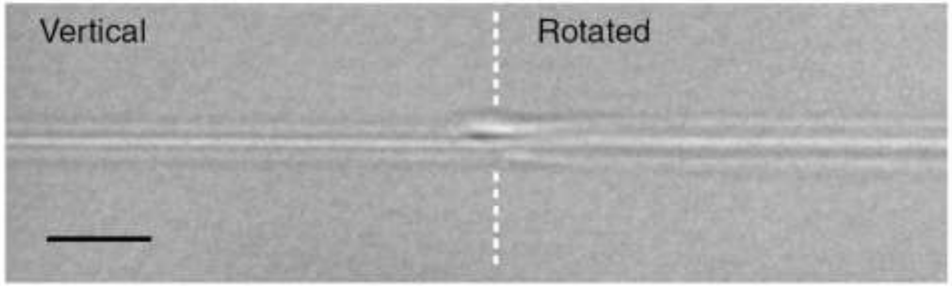

- Writing with **successive laser scans**, we can join a waveguide with vertical axis with a waveguide with tilted axis, **forming different waveplate combinations.**

- We demonstrated a photonic chip for polarization tomography of photonic qubits.

CHIP FOR POLARIZATION STATE TOMOGRAPHY

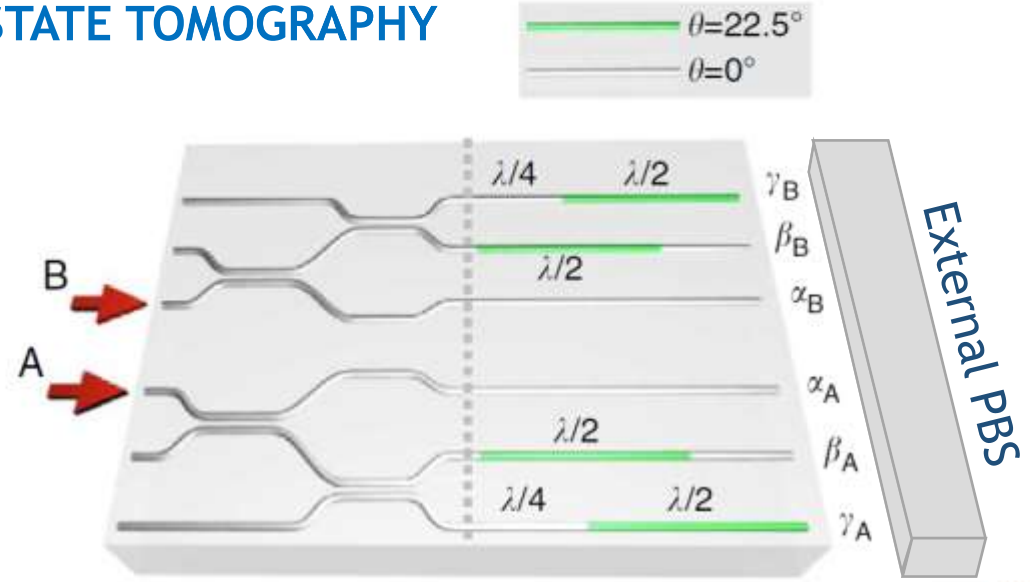

CHARACTERIZATION OF A POLARIZATION ENTANGLED PHOTON STATE

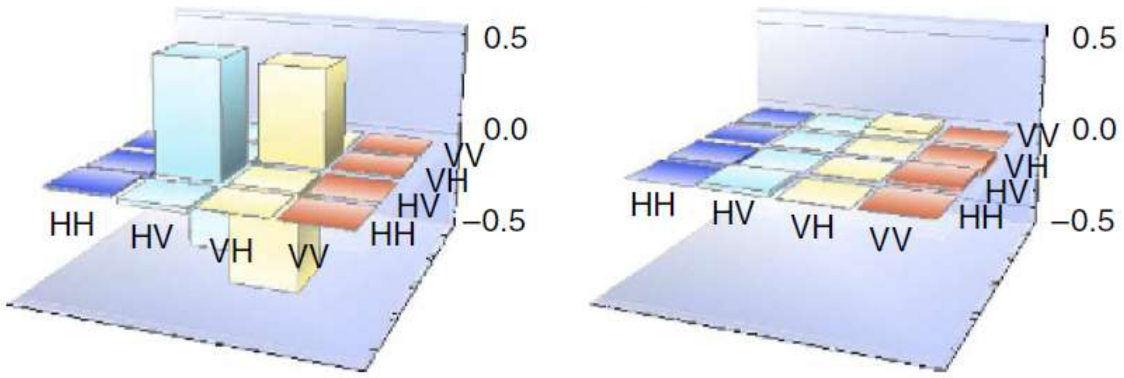

G. Corrielli, et al. *Nat. Commun.* 5, 4249 (2014).

POLITECNICO MILANO 1863 CNR IFN Istituto di Fotonica e Nanotecnologie SAPIENZA UNIVERSITÀ DI ROMA

Outline

1. Photons and qubits

2. Integrated quantum photonics

How a linear interaction can become nonlinear… and elaborate information.

3. Computing with linear optics

4. Boson sampling and complex interferometers

The beam splitter: a classic

A beam splitter enforces **a linear interaction** between two optical modes.

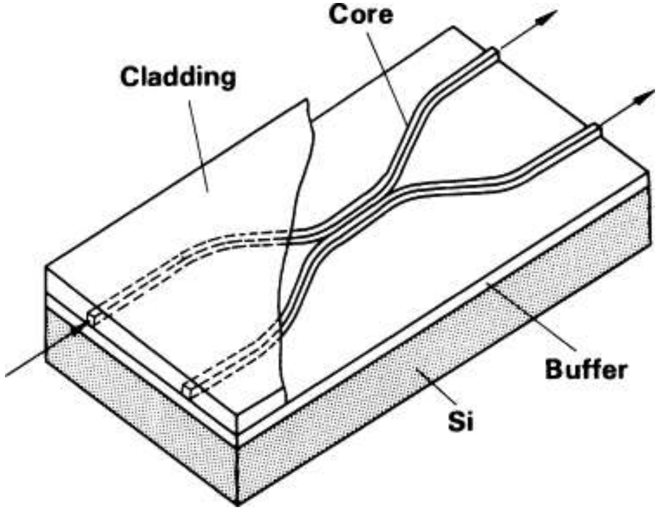

The integrated-optics beam splitter is the **directional coupler**: two waveguides exchange power by evanescent-field interaction.

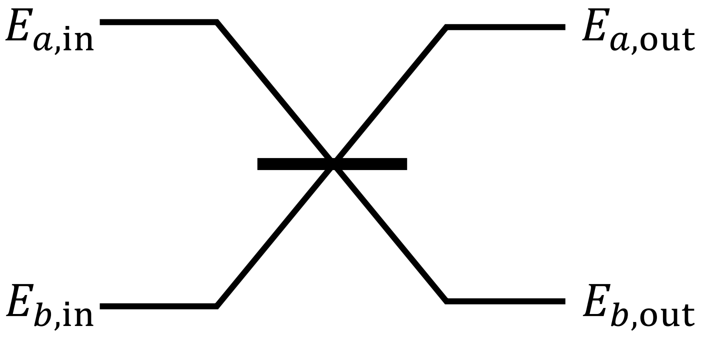

In the **classical picture**, we can relate the electric field phasors of the input and output modes as:

unitary matrix

$$\begin{bmatrix} E_{a,\mathrm{out}} \\ E_{b,\mathrm{out}} \end{bmatrix} = \begin{bmatrix} t & jr \\ jr^* & t \end{bmatrix} \begin{bmatrix} E_{a,\mathrm{in}} \\ E_{b,\mathrm{in}} \end{bmatrix} = M \begin{bmatrix} E_{a,\mathrm{in}} \\ E_{b,\mathrm{in}} \end{bmatrix}$$

$$|t|^2 + |r|^2 = 1$$

A single photon split?

The quantum model replaces the relation between the phasors with a relation between **annihilation operators** belonging to the input and output modes.

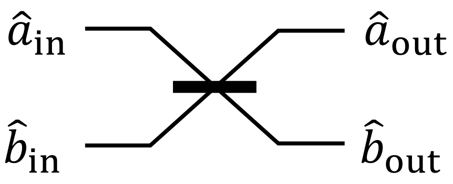

$$\begin{bmatrix}\hat{a}_{\text{out}}\\ \hat{b}_{\text{out}}\end{bmatrix} = \begin{bmatrix} t & jr \\ jr^* & t\end{bmatrix}\begin{bmatrix}\hat{a}_{in}\\ \hat{b}_{\text{in}}\end{bmatrix} = M\begin{bmatrix}\hat{a}_{in}\\ \hat{b}_{\text{in}}\end{bmatrix}$$

same matrix M of the classical model

Which is to say:

$$\begin{bmatrix}\hat{U}_{\text{BS}}^{\dagger}\,\hat{a}\,\hat{U}_{\text{BS}}\\ \hat{U}_{\text{BS}}^{\dagger}\,\hat{b}\,\hat{U}_{\text{BS}}\end{bmatrix} = M\begin{bmatrix}\hat{a}\\ \hat{b}\end{bmatrix}$$

evolved operators in the Heisenberg picture

EVOLUTION OF A SINGLE-PHOTON STATE

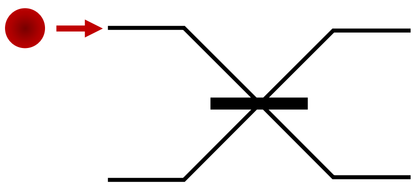

$$\hat{U}_{\text{BS}}|\emptyset\rangle = |\emptyset\rangle \Leftrightarrow \hat{U}^{\dagger}{}_{\text{BS}}|\emptyset\rangle = |\emptyset\rangle$$

$$|\psi_{\text{in}}\rangle = |1\emptyset\rangle = \hat{a}^{\dagger}\,|\emptyset\rangle$$

$$|\psi_{\text{out}}\rangle = \hat{U}_{BS}\,|1\emptyset\rangle = \hat{U}_{BS}\,\hat{a}^{\dagger}|\emptyset\rangle = \hat{U}_{\text{BS}}\hat{a}^{\dagger}\underbrace{\hat{U}_{\text{BS}}^{\dagger}}|\emptyset\rangle =$$

$$= \underbrace{\left(t\,\hat{a}^{\dagger} + jr^*\,\hat{b}^{\dagger}\right)}|\emptyset\rangle = t\,|1\emptyset\rangle + jr^*|\emptyset 1\rangle$$

$$\begin{bmatrix}\hat{U}_{\text{BS}}\,\hat{a}^{\dagger}\,\hat{U}_{\text{BS}}^{\dagger}\\ \hat{U}_{\text{BS}}\,\hat{b}^{\dagger}\,\hat{U}_{\text{BS}}^{\dagger}\end{bmatrix} = M^{\text{T}}\begin{bmatrix}\hat{a}^{\dagger}\\ \hat{b}^{\dagger}\end{bmatrix}$$

path-entangled single-photon state

Two-photon interference

EVOLUTION OF A SYMMETRIC TWO PHOTON STATE

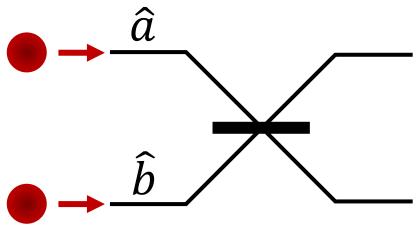

$$M = \frac{\sqrt{2}}{2}\begin{bmatrix} 1 & j \\ j & 1 \end{bmatrix}$$

balanced BS

$$|\psi_{\text{in}}\rangle = |11\rangle = \hat{a}^\dagger \hat{b}^\dagger |\emptyset\rangle$$

we transform the two operators

the $|11\rangle$ output is suppressed by quantum interference!

$$|\psi_{\text{out}}\rangle = \overbrace{\hat{U}_{\text{BS}}\ \hat{a}^\dagger\ \hat{U}_{\text{BS}}^\dagger}\ \overbrace{\hat{U}_{\text{BS}}\ \hat{b}^\dagger\ \hat{U}_{\text{BS}}^\dagger}|\emptyset\rangle = \frac{1}{2}\left(\hat{a}^\dagger + j\hat{b}^\dagger\right)\left(j\hat{a}^\dagger + \hat{b}^\dagger\right)|\emptyset\rangle =$$

$$= j\,\frac{\hat{a}^{\dagger 2} + \hat{b}^{\dagger 2}}{2}|\emptyset\rangle + \frac{\cancel{\hat{a}^\dagger \hat{b}^\dagger} - \cancel{\hat{a}^\dagger \hat{b}^\dagger}}{2}|\emptyset\rangle = j\,\frac{|2\emptyset\rangle + |\emptyset 2\rangle}{\sqrt{2}}$$

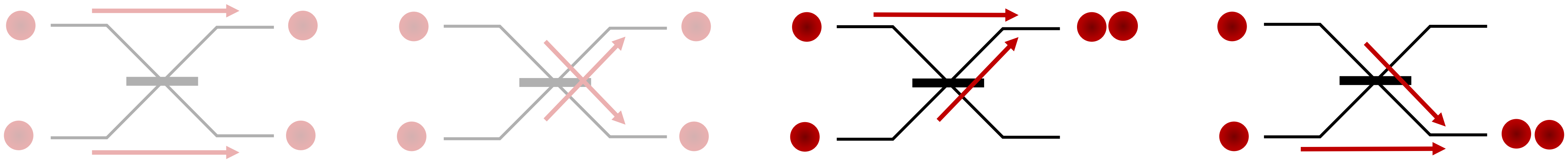

NO **NO** **YES** **YES**

C.K. Hong, Z.Y. Ou, & L. Mandel *Phys. Rev. Lett.* 59, 2044 (1987)

An artificial nonlinear phase

SINGLE-PHOTON INPUT

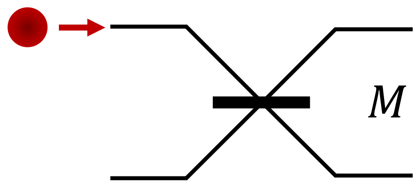

$$M = \begin{bmatrix} t & jr \\ jr & t \end{bmatrix}$$

$$|1\varnothing\rangle = \hat{a}^\dagger|\varnothing\rangle \rightarrow \left(t\,\hat{a}^\dagger + jr\,\hat{b}^\dagger\right)|\varnothing\rangle = \underline{t\,|1\varnothing\rangle} + jr|\varnothing 1\rangle$$

SYMMETRIC TWO-PHOTON INPUT

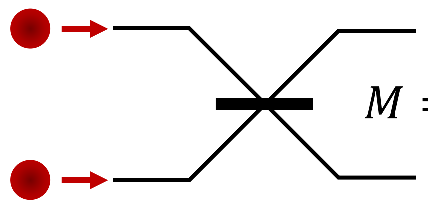

$$M = \begin{bmatrix} t & jr \\ jr & t \end{bmatrix}$$

$$|11\rangle = \hat{a}^\dagger\hat{b}^\dagger|\varnothing\rangle \rightarrow \left(t\,\hat{a}^\dagger + jr\,\hat{b}^\dagger\right)\left(jr\,\hat{a}^\dagger + t\,\hat{b}^\dagger\right)|\varnothing\rangle =$$
$$= jrt\left(\hat{a}^{\dagger 2} + \hat{b}^{\dagger 2}\right)|\varnothing\rangle + (t^2 - r^2)\,\hat{a}^\dagger\,\hat{b}^\dagger|\varnothing\rangle =$$
$$= jrt\sqrt{2}(|2\varnothing\rangle + |\varnothing 2\rangle) + \underline{(t^2 - r^2)|11\rangle}$$

Post-selection of 1-photon states on mode a:
if $r^2 > t^2$, e.g. $r^2 = {}^2/_3 \quad t^2 = {}^1/_3$

phase 0

$$t|10\rangle = +\frac{\sqrt{3}}{3}|10\rangle$$

$$(t^2 - r^2)|11\rangle = -\frac{1}{3}|11\rangle$$

phase π

The presence of the other photon imparts a phase shift on the state.

THE KEY ELEMENT IS POST-SELECTION

THE PHASE SHIFT CAN BE EXPLOITED IN A SUITABLE INTERFEROMETER

The photonic CNOT gate (1)

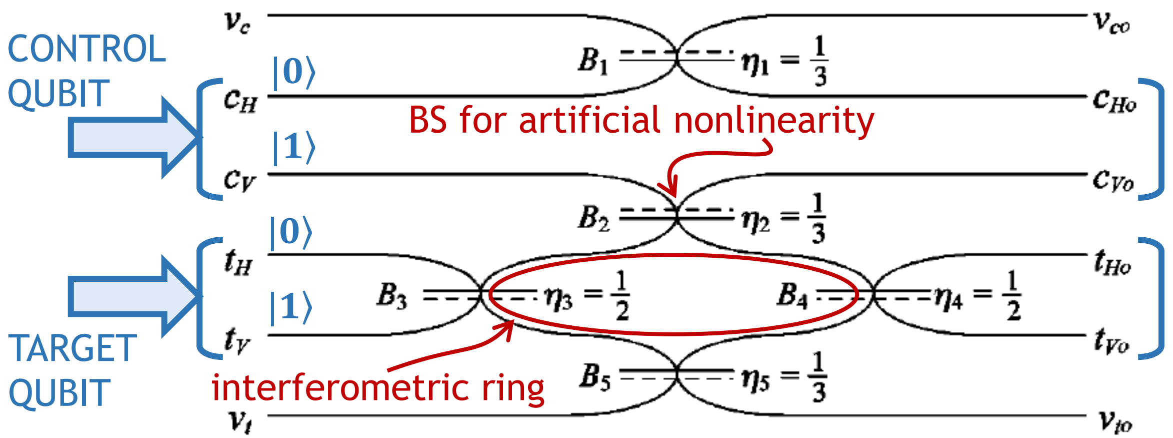

T.C. Ralph et al. "Linear optical controlled-NOT gate in the coincidence basis." *Phys. Rev. A* 65, 062324 (2002).

- One fundamental quantum logic gate is the CNOT (controlled not). It inverts the Target qubit when the Control qubit is 1. Differently from classical logic gates it can operate on superposition states.

$$\hat{U}_{\mathrm{CNOT}} = |\mathbf{00}\rangle\langle\mathbf{00}| + |\mathbf{01}\rangle\langle\mathbf{01}| + \\ + |\mathbf{11}\rangle\langle\mathbf{10}| + |\mathbf{10}\rangle\langle\mathbf{11}|$$

- A photonic CNOT gate using linear optics can be realized by properly enclosing the artificial nonlinearity in a Mach-Zehnder ring.

- First demonstrated with bulk optics, in 2008 a **photonic CNOT gate** was demonstrated in a waveguide device, using path encoding.

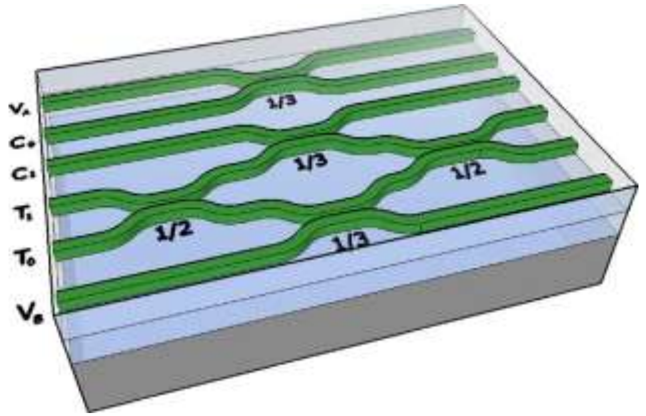

A. Politi et al. "Silica-on-silicon waveguide quantum circuits. " *Science 320*, 646-649 (2008).

The photonic CNOT gate (2)

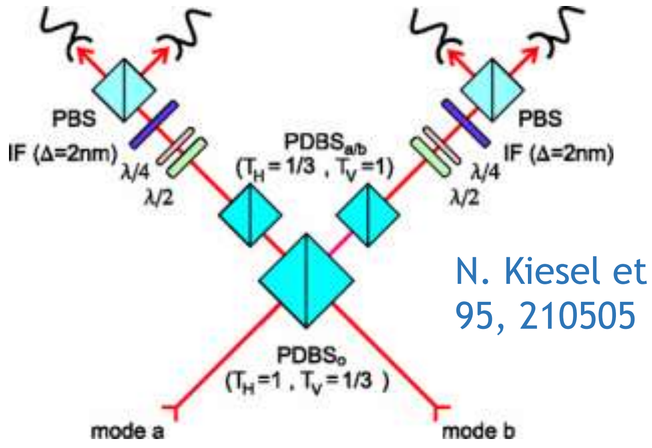

N. Kiesel et al. *Phys. Rev. Lett.* 95, 210505 (2005).

- A polarization encoded CNOT gate requires **three partially-polarizing beam splitters (PPBS).**

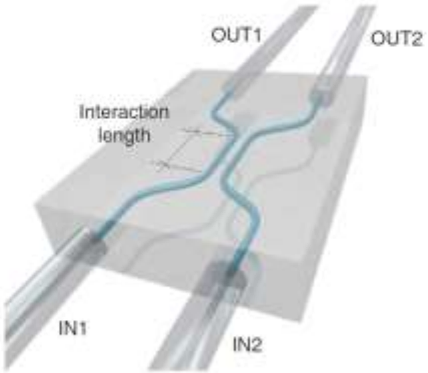

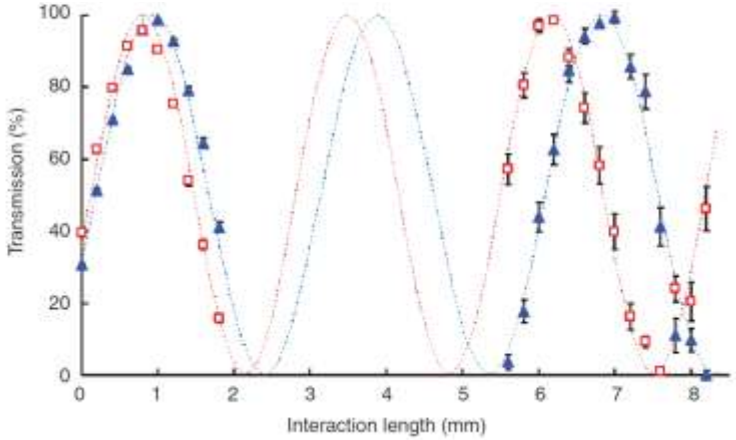

- Thanks to the controlled waveguide birefringence, **femtosecond laser written directional couplers** are indeed PPBS. The interaction length tunes the splitting ratio.

A. Crespi et al. *Nat. Commun.* 2, 566 (2011).

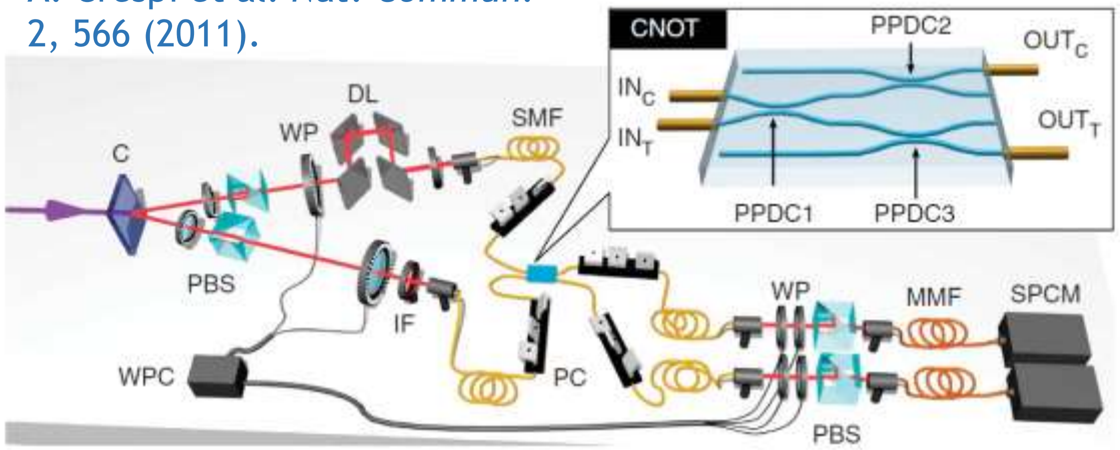

- **We could integrate on-chip a polarization-encoded CNOT gate.**

POLITECNICO MILANO 1863
CNR IFN Istituto di Fotonica e Nanotecnologie
SAPIENZA UNIVERSITÀ DI ROMA

Outline

1. Photons and qubits
2. Integrated quantum photonics
3. Computing with linear optics
4. Boson sampling and complex interferometers

Going beyond photonic quantum logic gates

Boson sampling: the concept (1)

$$|G\rangle = |g_1 g_2 \cdots g_m\rangle = \prod_{i=1}^{m} \frac{(\hat{a}^\dagger)^{g_i}}{g_i!} |\emptyset\rangle$$

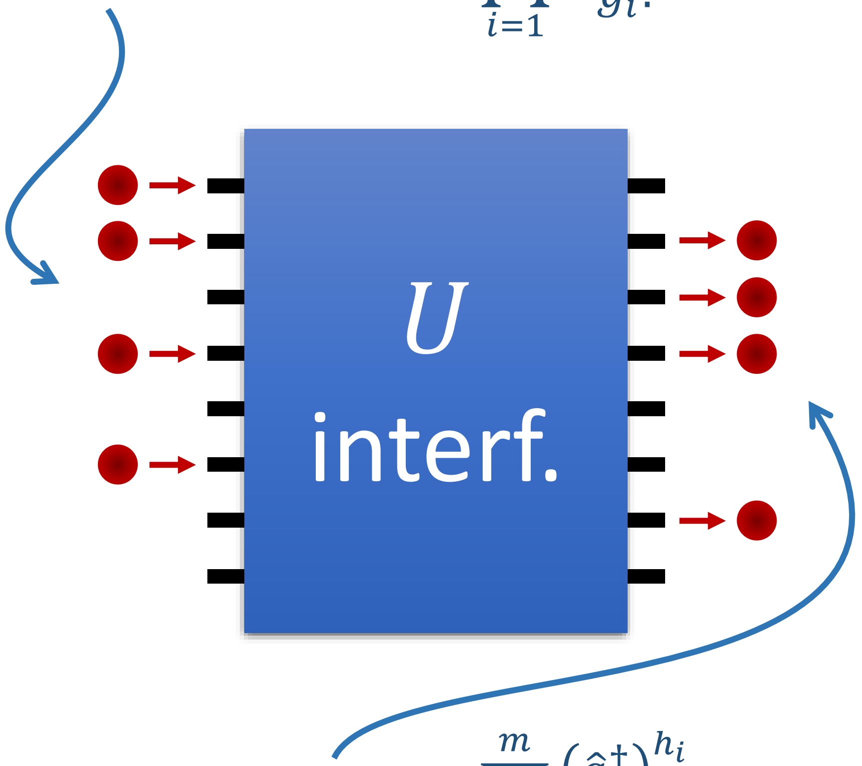

$$|H\rangle = |h_1 h_2 \cdots h_m\rangle = \prod_{i=1}^{m} \frac{(\hat{a}^\dagger)^{h_i}}{h_i!} |\emptyset\rangle$$

THEOREM

We consider a $m \times m$ multi-port interferometer, described by a unitary matrix U. The probability associated with input $|G\rangle = |g_1 g_2 \cdots g_m\rangle$ and output $|H\rangle = |h_1 h_2 \cdots h_m\rangle$ is given by

$$p_{G\to H} = \frac{\left|\mathrm{perm}(U_{G,H})\right|^2}{g_1!\, g_2! \cdots g_m!\, h_1!\, h_2! \cdots h_m!}$$

where $U_{G,H}$ is the matrix obtained by repeating g_i times the i-th row of U and h_j times its j-th column.

S. Scheel "Permanents in linear optical networks " *arXiv preprint quant-ph/0406127* (2004).
S. Aaronson & A. Arkhipov. "The computational complexity of linear optics“ *Proc. of the 43rd annual ACM symposium on Theory of computing* (2011).

Boson sampling: the concept (2)

$$p_{G\rightarrow H} = \frac{\left|\mathrm{perm}(U_{G,H})\right|^2}{g_1!\, g_2! \cdots g_m!\, h_1!\, h_2! \cdots h_m!}$$

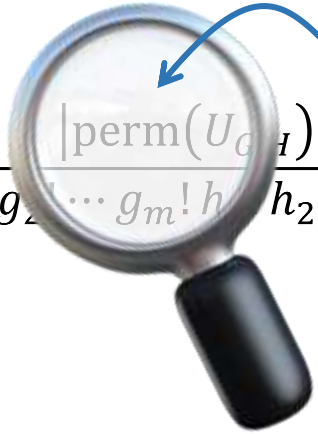

The permanent is a 'determinant with only plus signs'.

$$\det(U) = \sum_{\sigma\in S_n} \mathrm{sgn}(\sigma)\, u_{1,\sigma_1} u_{2,\sigma_2} \cdots u_{m,\sigma_m}$$

$$\mathrm{perm}(U) = \sum_{\sigma\in S_n} +\, u_{1,\sigma_1} u_{2,\sigma_2} \cdots u_{m,\sigma_m}$$

The determinant can be calculated **efficiently** by a classical computer; permanent instead is conjectured to be **hard to compute** (i.e. calculation time scales exponentially with matrix size).

Matrix size	19	20	21	22	23
Permanent calculation time	3,2 s	6,5 s	13 s	27 s	58 s

Look how badly it scales!

TASK: producing 'samples' from the output boson distributions, given a random *U*

A physical experiment (i.e. the quantum hardware) could be much faster than a classical computer that simulates it. This is a **viable route to demonstrate a real quantum advantage.**

BOSON SAMPLING

Boson sampling: the race

- A boson sampling experiment can be ‘readily’ performed with photons, linear optics and single photon detectors.
- A worldwide scientific race started, towards reaching **sufficiently many modes** (maybe easy) and **sufficiently many identical photons** (not easy at all!) to arrive to a complexity regime inaccessible to computers.

2013 - First four photonic boson sampling experiments

2020 – QUANTUM ADVANTAGE by boson sampling

As a matter of fact, to get the ‘quantum’… a lot of ‘classical’ is needed…

Science 370, 1460-1463 (2020)

Arbitrary multimode interferometers

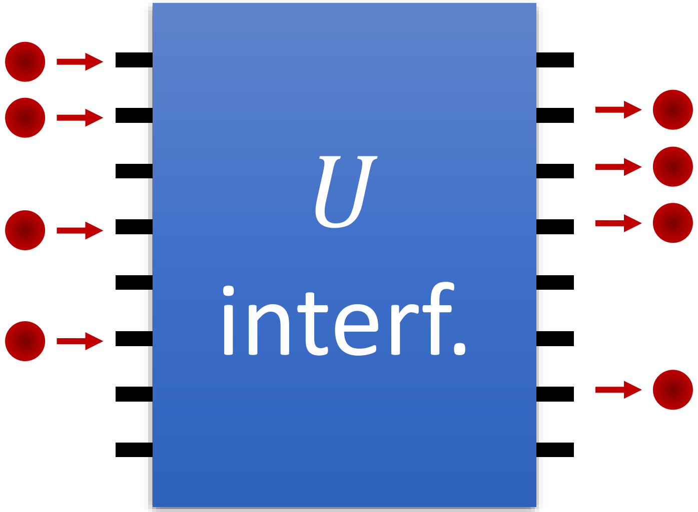

Is it possible to realize a multimode interferometer described by an arbitrary unitary matrix *U*?

DECOMPOSITIONS WITH BEAM SPLITTER NETWORKS

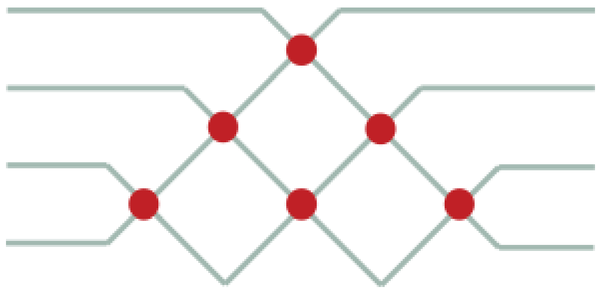

Reck et al., *Phys. Rev. Lett.* 73, 58-61 (1994).

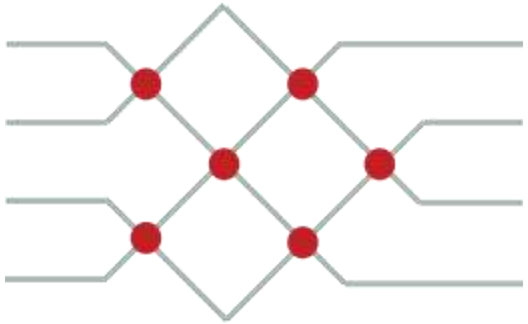

Clements et al., *Optica* 3, 1460-1465 (2016).

BOTH CAN SHARE THE SAME BASIC CELL ( )

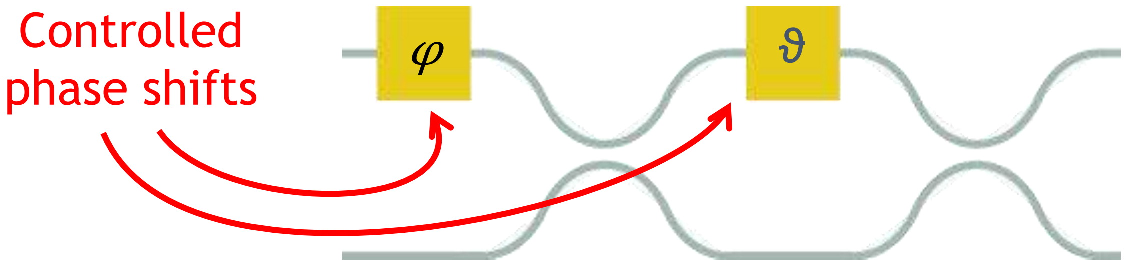

A Mach-Zehnder interferometer can act as a variable beam splitter.

Reconfiguring integrated optics (1)

INTEGRATED PROGRAMMABLE BEAM SPLITTER

- A resistive microheater heats up the target waveguide by Joule effect
- The thermo-optic effect is exploited to induce the desired phase shift

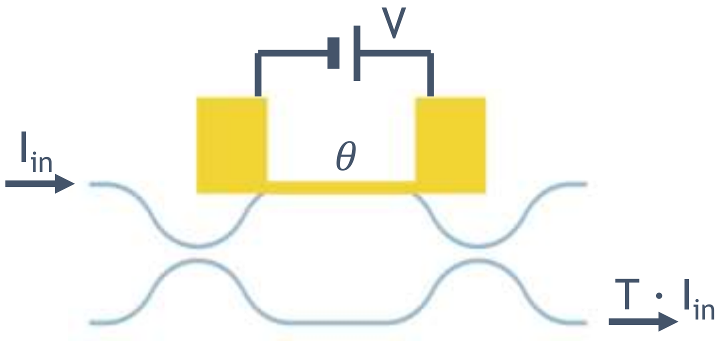

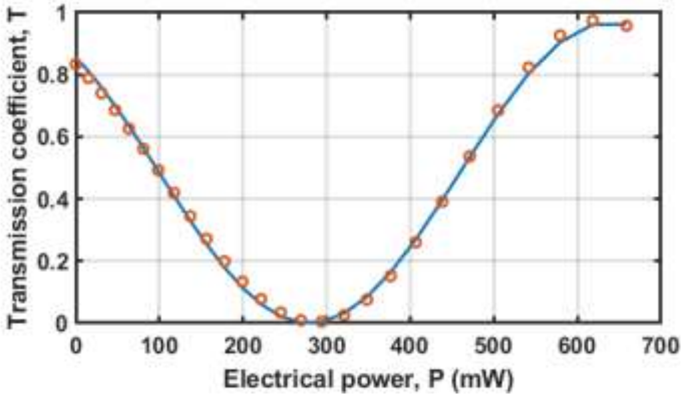

THERMAL SHIFTER FABRICATION

1. Gold sputtering/evaporation

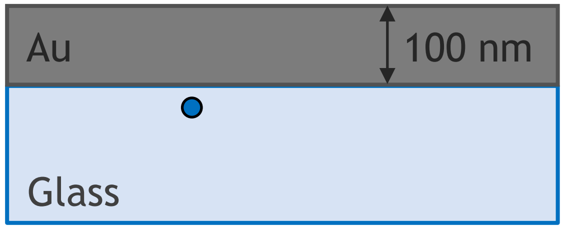

2. Thermal annealing

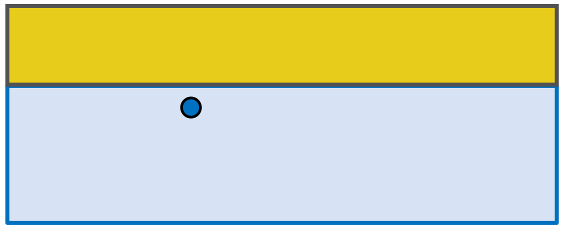

annealing step required for enhanced stability and reliability

3. fs laser patterning

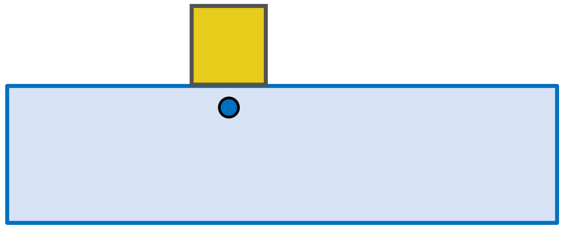

F. Flamini et al. *Light Sci Appl* 4, e354 (2015).
F. Ceccarelli et al., *J. Light. Technol.* 37, 4265-4271 (2019).

Reconfiguring integrated optics (2)

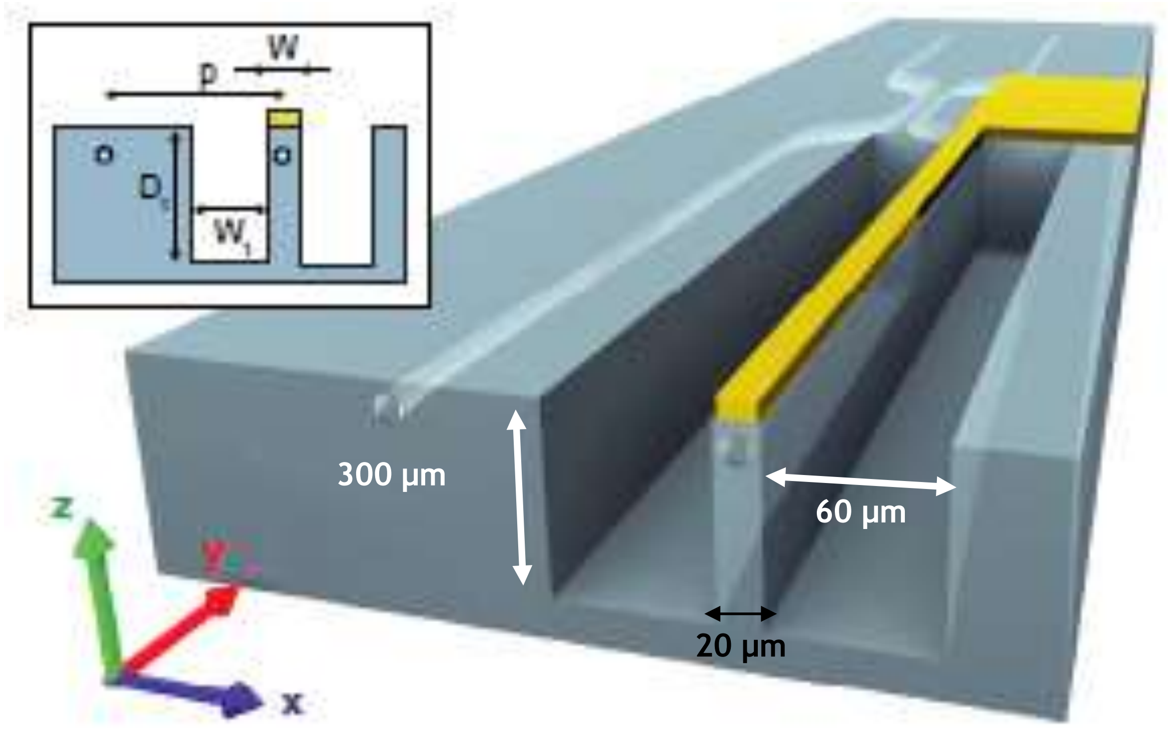

DEEP ISOLATION TRENCHES

- Fabrication via water-assisted laser ablation
- Drastic reduction in both power dissipation and thermal crosstalk
- Slowed down time response

Device (785 nm)	Power (2π)	Thermal crosstalk	Time response
Planar	425 mW	< 70 %	10 ms
Trenches	32 mW	< 30%	45 ± 10 ms

F. Ceccarelli et al. Laser Photon. Rev. 14, 2000024 (2020).

A femtosecond-laser-written UPC (1)

6 MODE UNIVERSAL PHOTONIC PROCESSOR

- Deep isolation trenches (300 µm deep)
- Rectangular mesh configuration
- 6 modes, 30 thermal phase shifters
- 2.7 dB total insertion loss (<u>λ = 785 nm</u>)

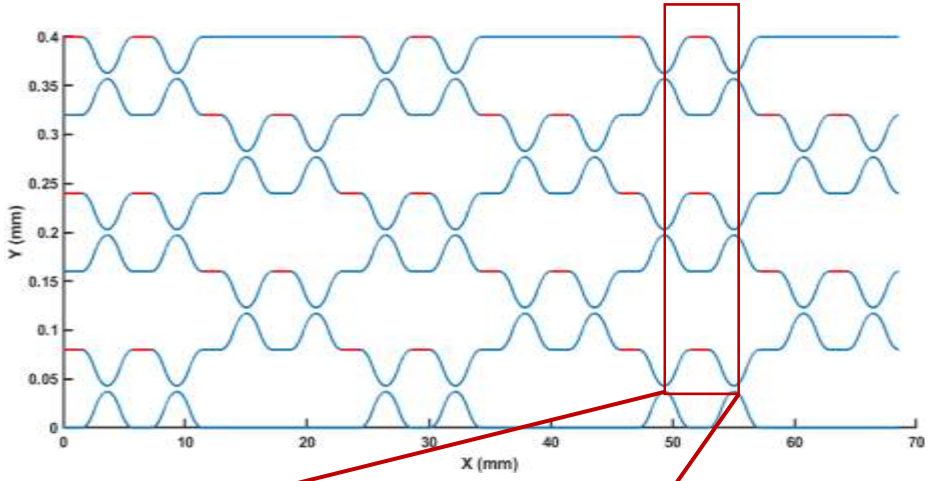

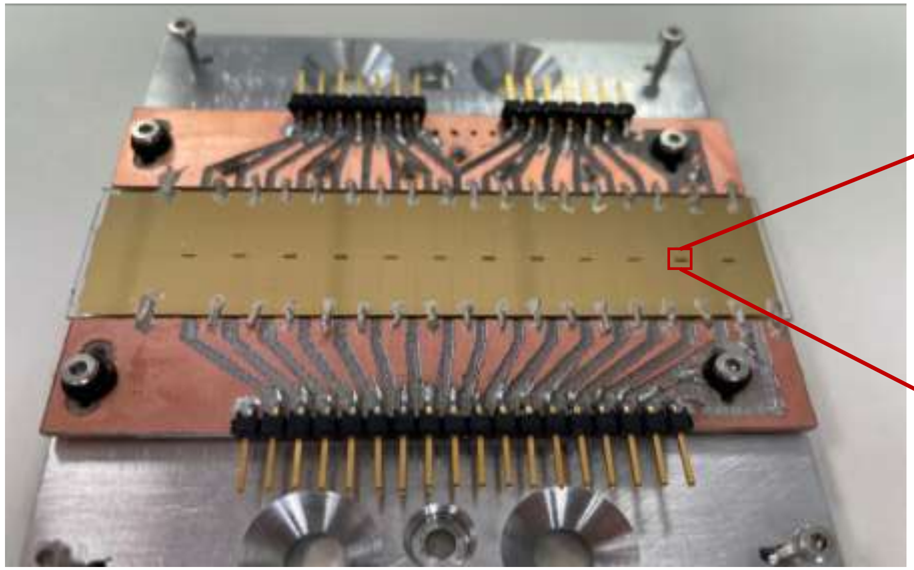

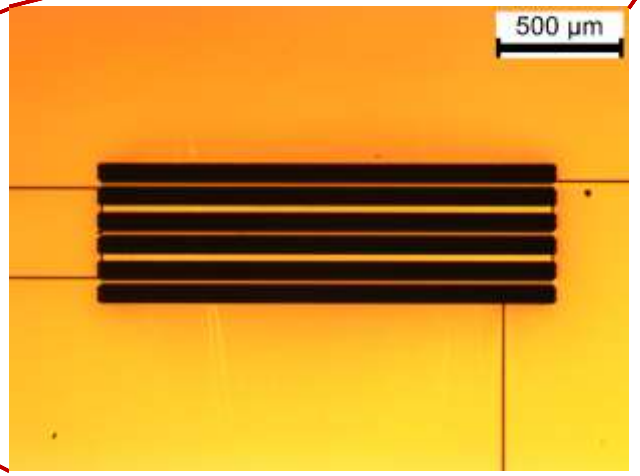

C. Pentangelo et al. "Universal photonic processors fabricated by femtosecond laser writing." *Integrated Optics: Devices, Materials, and Technologies XXVI*. Vol. 12004. SPIE, 2022.

A femtosecond-laser-written UPC (2)

Full calibration performance evaluated by implementing Haar-random unitary matrices

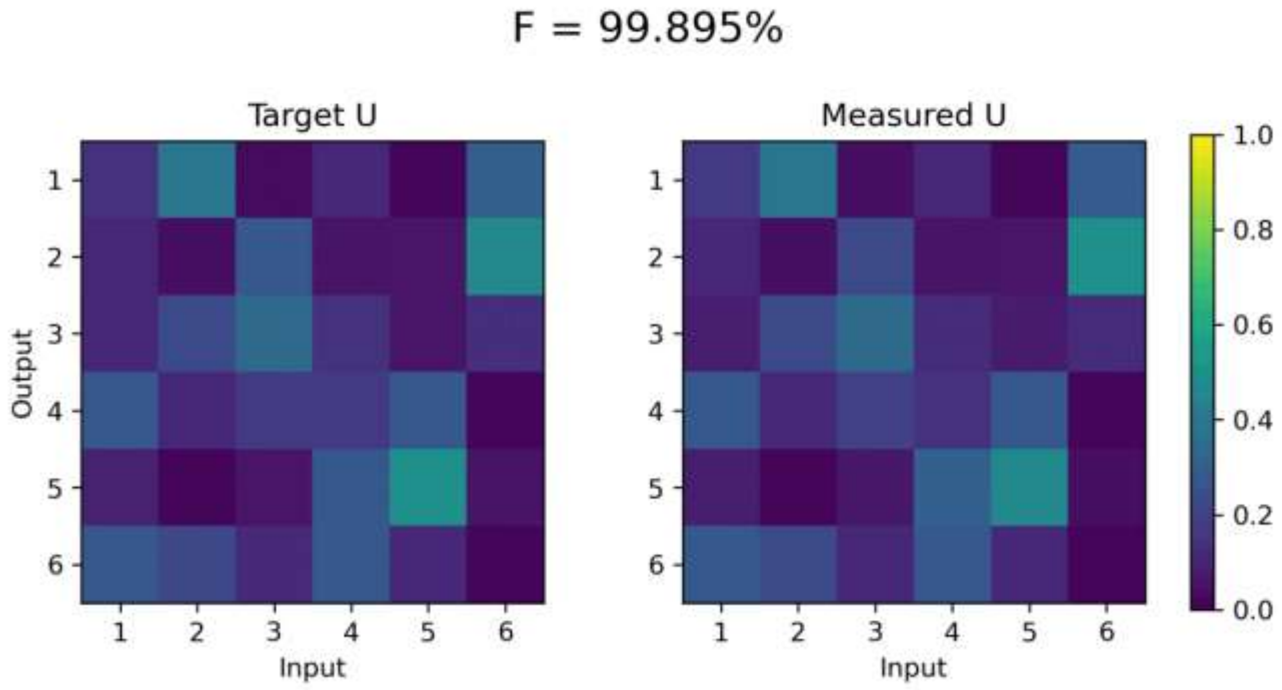

Measured: 1000
Avg. Fidelity ($F_{avg} \pm \sigma$):
0.9979 ± 0.0008

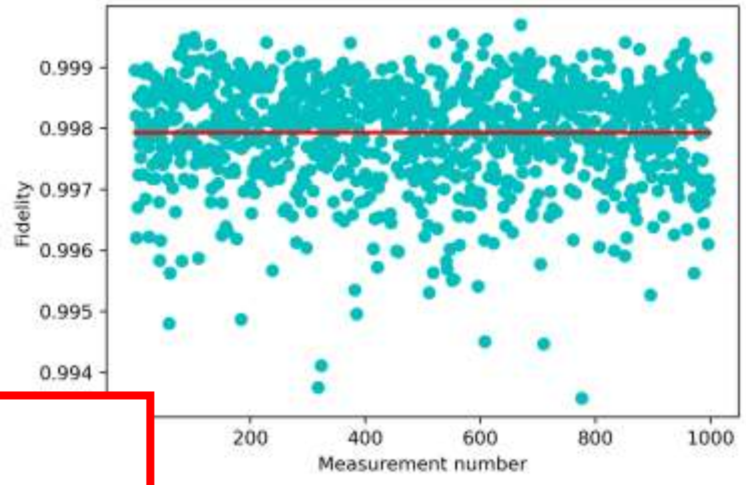

WE ARE READY FOR QUANTUM EXPERIMENTS!

C. Pentangelo et al. "Universal photonic processors fabricated by femtosecond laser writing." *Integrated Optics: Devices, Materials, and Technologies XXVI*. Vol. 12004. SPIE, 2022.

Other recent milestones(1)

2019 – Proved the possibility to interface a fs laser written photonic circuit with a quantum-dot single photon source.

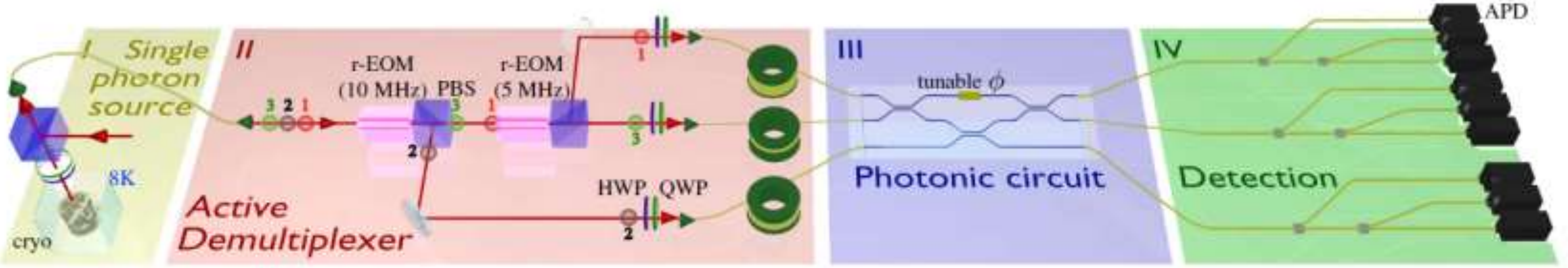

C. Antón et al. "Interfacing scalable photonic platforms: solid-state based multi-photon interference in a reconfigurable glass chip." *Optica* 6, 1471-1477 (2019).

2022 – Developed a reliable test, based on a new kind of interferometer, to ascertain the indistinguishability of the photons (essential to achieve quantum tasks).

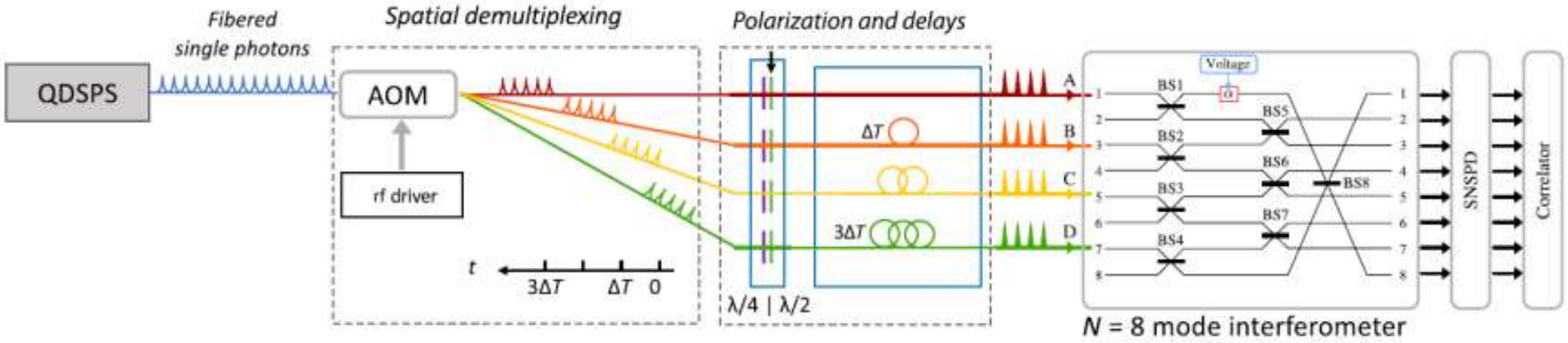

M. Pont et al. "Quantifying n-photon indistinguishability with a cyclic integrated interferometer." Phys. Rev. X 12, 031033 (2022).

Other recent milestones(2)

2022 – Boson sampling experiment in a **reconfigurable three-dimensional waveguide array.**

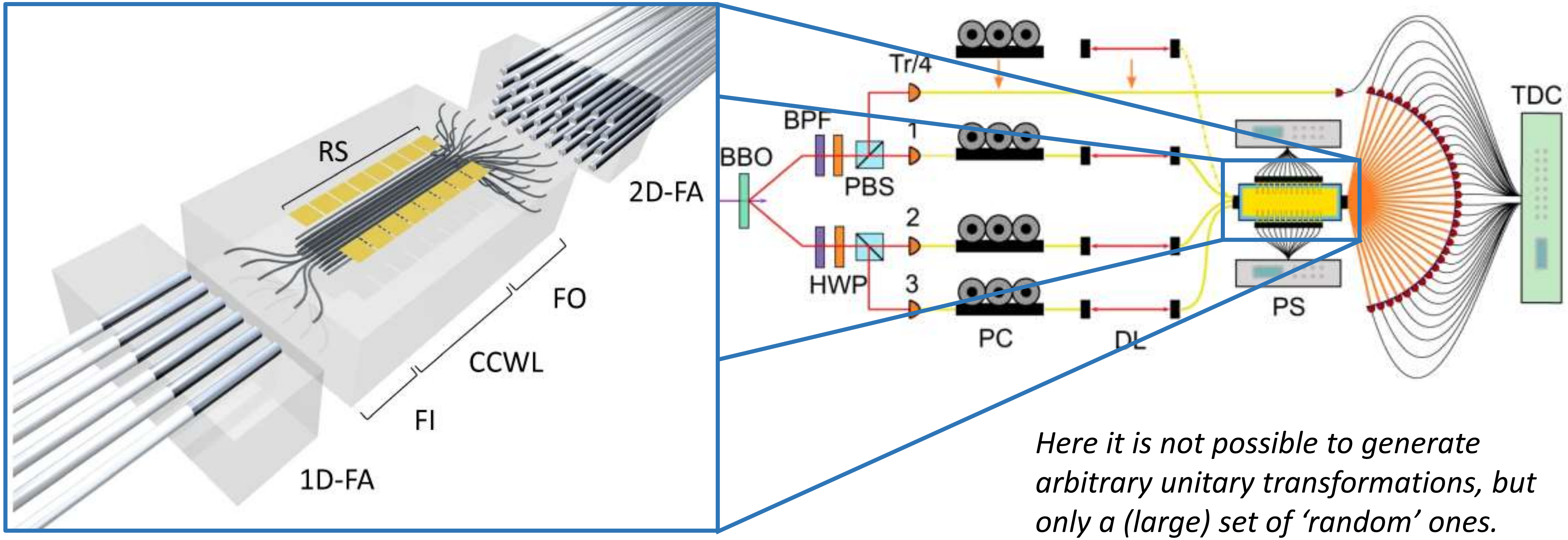

Here it is not possible to generate arbitrary unitary transformations, but only a (large) set of 'random' ones.

F. Hoch et al. "Reconfigurable continuously-coupled 3D photonic circuit for Boson Sampling experiments " *npj Quantum Inf* **8**, 55 (2022).

Conclusions

- I hope I have convinced you that:
  - ➢ Qubits can be conveniently encoded on photons.
  - ➢ Linear optics is good.
  - ➢ Integrated optics is… better!
- And… you should follow us on Twitter!

  @fastgroup_ifn